JOURNAL OF GENERAL VIROLOGY

RESEARCH ARTICLE

James *et al.*, *Journal of General Virology*

DOI 10.1099/jgv.0.001220

MICROBIOLOGY SOCIETY

OPEN MICROBIOLOGY

The cellular localization of avian influenza virus PB1-F2 protein alters the magnitude of IFN2 promoter and NFκB-dependent promoter antagonism in chicken cells

Joe James,[1,2]† Nikki Smith,[3] Craig Ross,[4] Munir Iqbal,[1] Steve Goodbourn,[4] Paul Digard,[3] Wendy S. Barclay[2] and Holly Shelton[1,*]

Abstract

The accessory protein, PB1-F2, of influenza A virus (IAV) functions in a chicken host to prolong infectious virus shedding and thus the transmission window. Here we show that this delay in virus clearance by PB1-F2 in chickens is accompanied by reduced transcript levels of type 1 interferon (IFN)-induced genes and NFκB-activated pro-inflammation cytokines. *In vitro*, two avian influenza isolate-derived PB1-F2 proteins, H9N2 UDL01 and H5N1 5092, exhibited the same antagonism of the IFN and pro-inflammation induction pathways seen *in vivo*, but to different extents. The two PB1-F2 proteins had different cellular localization in chicken cells, with H5N1 5092 being predominantly mitochondrial-associated and H9N2 UDL being cytoplasmic but not mitochondrial-localized. We hypothesized that PB1-F2 localization might influence the functionality of the protein during infection and that the protein sequence could alter cellular localization. We demonstrated that the sequence of the C-terminus of PB1-F2 determined cytoplasmic localization in chicken cells and this was linked with protein instability. Mitochondrial localization of PB1-F2 resulted in reduced antagonism of an NFκB-dependent promoter. In parallel, mitochondrial localization of PB1-F2 increased the potency of chicken IFN 2 induction antagonism. We suggest that mitochondrial localization of PB1-F2 restricts interaction with cytoplasmic-located IKKβ, reducing NFκB-responsive promoter antagonism, but enhances antagonism of the IFN2 promoter through interaction with the mitochondrial adaptor MAVS. Our study highlights the differential mechanisms by which IAV PB1-F2 protein can dampen the avian host innate signalling response.

INTRODUCTION

Influenza A viruses (IAVs) are respiratory pathogens of multiple species, including poultry and humans. The high prevalence levels of IAV infection in poultry in the Middle East and South-East Asia, where it is considered to be endemic in some countries, are a significant economic burden to the poultry industry [1, 2]. It is estimated that the H7N9 subtype of avian IAV caused upwards of $6.5 billion in losses to the Chinese economy in 2013 alone [3]. Food security, animal welfare and of course the potential spillover into the human population and the resulting possibility of pandemics, are all important reasons for further study of IAV interactions within avian hosts, with the aim of enabling the design and implementation of better control strategies for IAV in poultry.

IAVs have a core repertoire of 10 viral proteins that all subtypes express, allowing successful replication of the virus in infected cells. There is also an ever increasing number of 'accessory' proteins that are not required for replication in a cell, but which contribute and modulate IAV infection *in vivo* [4]. In 2001, PB1-F2 was the first accessory protein to be identified in IAV [5]. PB1-F2 is a small protein that ranges in size from 87 to 101 amino acids (aa) and is expressed from genome segment 2 of IAV in a +1 reading

Received 17 September 2018; Accepted 25 December 2018; Published 23 January 2019

Author affiliations: [1]The Pirbright Institute, Pirbright, Woking, UK; [2]Imperial College London, London, UK; [3]The Roslin Institute, Edinburgh, UK; [4]St George's, University of London, London, UK.

***Correspondence:** Holly Shelton, holly.shelton@pirbright.ac.uk

Keywords: influenza virus; PB1-F2; IKKβ; MAVS; chicken.

Abbreviations: aa, amino acid; BMDM, bone marrow derived macrophages; BSA, bovine serum albumin; cCSF-1, chicken colony stimulating factor 1; CEF, chicken embryo fibroblasts; CKC, chicken kidney cells; DF-1, doug foster-1; ELISA, enzyme linked immunosorbent assay; EMEM, eagle's minimum essential media; FBS, foetal bovine serum; GFP, green fluorescent protein; HEK, human embryo fibroblasts; IAV, Influenza A Virus; IFN, interferon; IFNβ, interferon beta; ISG, interferon stimulated genes; MAVS, mitochondrial antiviral signalling protein ; MDCK, Madin-Darby canine kidney; NIH, National Institutes of Health; ORF, open reading frame; PBS, phosphate buffered saline; PRR, pathogen recognition receptor; VSV, vesicular stomatitis virus.

†**Present address:** APHA, Weybridge, UK.

Four supplementary figures are available with the online version of this article.

frame relative to that of the PB1 protein, the viral RNA-dependent RNA polymerase [5]. The presence of PB1-F2 in the IAV genome is highly conserved (93 %) as a full-length protein in IAV isolates recovered from avian species, which contrasts with a full-length conservation of only 43 % in human- or 48 % in swine-isolated IAV sequences [6, 7].

Many functions have been attributed to PB1-F2 since its identification; it has variously been shown to induce apoptosis, antagonize innate immune responses, promote secondary bacterial infection and modulate viral polymerase activity, but many of these functions have been shown to be cell type- and IAV strain-dependent [8, 9]. It has also been shown to be rapidly turned over in cells due to degradation by the proteosome [10].

Previously we and others have shown that the absence of a full-length PB1-F2 protein in an avian IAV has the effect of increasing pathogenicity in chickens, in both highly pathogenic and low-pathogenic IAV infection models [6, 11]. It has been documented in mammalian models that IAV infections with large innate responses, characterized by extraordinary levels of inflammatory cytokines and chemokines, correlate with enhanced pathogenicity [12, 13]. Therefore the absence of PB1-F2 resulting in enhanced innate immune responses is a likely mechanism for this increase in pathogenicity in chickens. It has previously been demonstrated in mammalian cells infected with IAV that PB1-F2 can antagonize anti-viral innate responses, for example Yoshizumi *et al.* and others report that human interferon beta (IFNβ) promoter activation is suppressed by the presence of PB1-F2 [14–17]. Additionally, *in vivo,* in mice, type 1 interferon (IFN)-induced transcripts in the lung were reduced when PB1-F2 was present [18]. In chickens, in the context of a highly pathogenic H5N1 IAV, it was found that similar to mice, infection with a virus that contained a full-length PB1-F2 protein resulted in reduced levels of a range of anti-viral innate gene transcripts [11]. A direct interaction between PB1-F2 of the vaccine strain A/PR/8/34 (PR8) and human mitochondrial antiviral signalling protein (MAVS) has been demonstrated by co-immunoprecipitation and it is thought that PB1-F2 exerts its antagonist function of mammalian IFNα/β through modulation of this critical adapter protein in the IFN induction pathway [19, 20]. Reis *et al.* showed that PB1-F2 from a range of avian IAVs and PR8 was able to interact with human IKKβ, resulting in the inhibition of human NFκB activation [18]. The antagonistic functionality of PB1-F2 for the interferon-induced and pro-inflammation pathways in avian cell lines and hosts is less clear, however, with only one study providing data where the effect of PB1-F2 on transcript levels of interferon-stimulated genes in the lungs of chickens infected with a highly pathogenic H5N1 strain was analysed [11]. Leymarie *et al.* showed that transcripts of the interferon signalling pathway were downregulated when they compared datasets from infections by a PB1-F2-containing virus and the isogenic knock-out of PB1-F2. Differences exist between the signalling induction pathways for innate response cytokines and chemokines in chickens and mammals; for example, chickens lack the pattern recognition receptor RIG-I, which is important for initiating the type 1 IFN induction pathway in mammals [21]. Sequence comparison between human MAVS and chicken MAVS shows only a 39 % conservation at the amino acid level, whereas there is a stronger degree of conservation between human IKKβ and that in the chicken genome (83 % conservation at amino acid level). There has been no analysis of the mechanism of immune response suppression in the chicken host by PB1-F2. It is likely that host immune response suppression results in the observation that our group previously reported, that the presence of a PB1-F2 protein in a low pathogenic H9N2 IAV can prolong the virus shedding duration in chickens, resulting in an increased transmission window and environmental contamination [6].

In mammalian cells, PB1-F2 proteins display one of two sub-cellular localizations; predominantly mitochondrial-associated, as is the case for the PB1-F2 protein from the laboratory-adapted H1N1 A/PR8/8/34 (PR8), or diffuse in the cytoplasm, with a small proportion of mitochondrial localization, as is the case for H5N1 A/HK/156/1997 [5, 22–25]. However, no study of cellular localization in avian cell types has been undertaken. It has been noted in several reports that the C-terminus sequence of the PB1-F2 protein determines cellular localization in mammalian cells, although the residues that confer mitochondrial targeting appear to vary between PB1-F2 proteins [22]. The ability of PB1-F2 to antagonize mammalian IFNα/β promoters has been linked to the C-terminus of PB1-F2 [19, 20].

The PB1-F2 protein of IAV is variable in sequence, which has been shown to impact on cellular localization and function in mammalian cells. There is a paucity of published information about PB1-F2 in the context of IAV infection of avian cells and IAV isolates that infect avian species are more likely to have a full-length PB1-F2 protein encoded in their genome. Therefore there is a particular gap in our knowledge of the specific *in vitro* functions of PB1-F2 in avian cells and how these might be correlated with the effects of PB1-F2 on IAV pathogenicity and viral shedding in chickens.

Here we analysed the cellular localization and ability of avian IAV PB1-F2 proteins to antagonize type 1 IFN (chicken IFN-1 and IFN-2) and pro-inflammation induction pathways in chicken cells. We demonstrated that the C-terminal sequence of PB1-F2 can alter the cellular localization and that mitochondrial association of PB1-F2 affects the antagonistic function and stability of PB1-F2 in chicken cells. We confirmed interactions with chicken orthologues of MAVs and IKKβ, suggesting that PB1-F2 acts to suppress innate responses in chickens and this is the mechanism of suppressed pathogenicity and prolonged viral shedding of IAV strains that carry full-length PB1-F2 proteins.

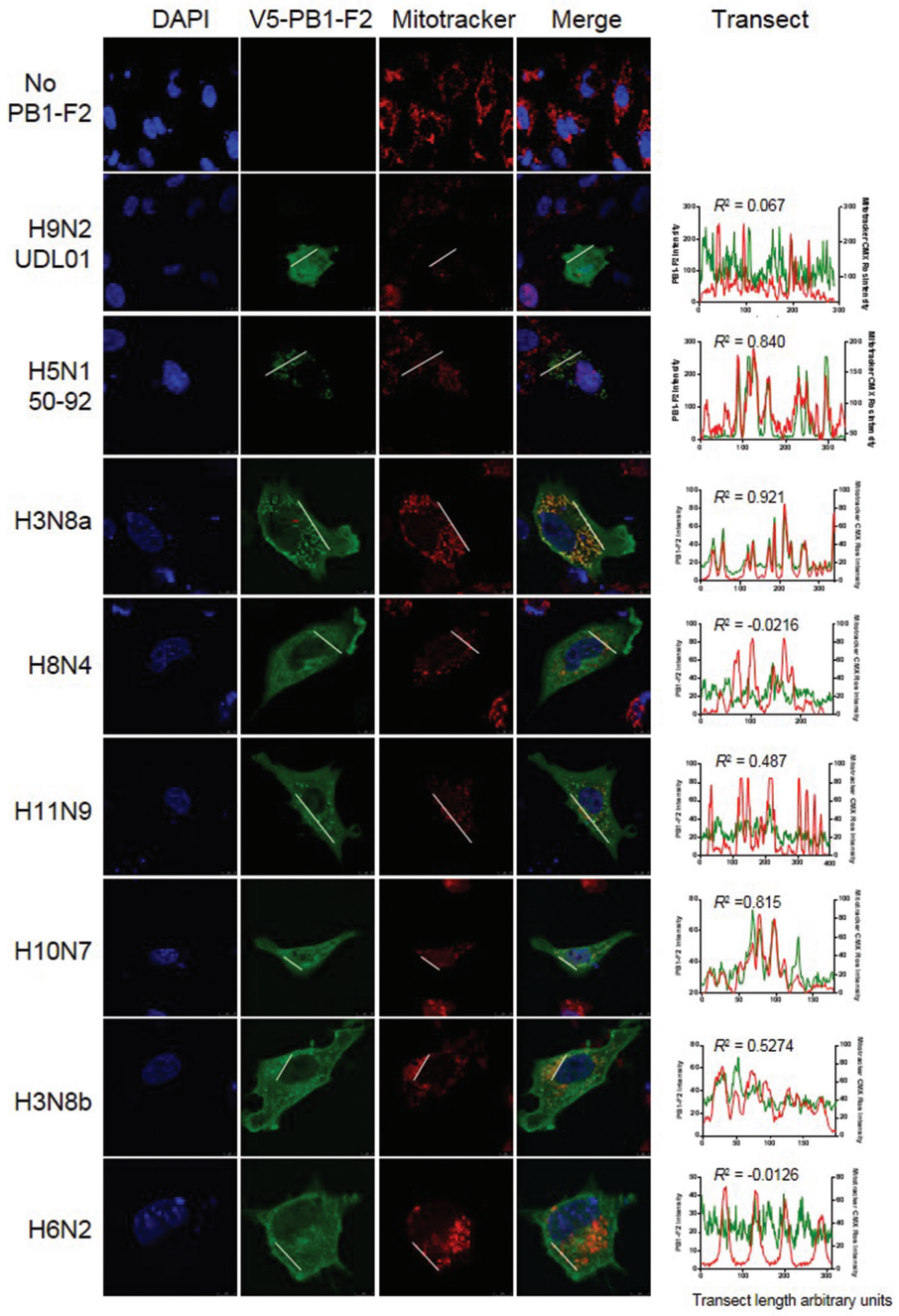

Fig. 1. PB1-F2 protein from avian influenza viruses have different subcellular locations in chicken cells. PB1-F2 proteins from a range of avian influenza subtypes were cloned into expression plasmids. DF-1 cells were transfected with V5-PB1-F2 expression plasmids and 12 h post-transfection stained with MitoTracker Red CMXRos [mitochondria (red)]. The cells were subsequently fixed and immunostained with an anti-V5 antibody [PB1-F2 (green)] and the nuclei were stained with DAPI [nucleus (Blue)]. Lines were drawn transecting objects in the 'red' channel (displayed as white lines) and the pixel intensities along these transects for both the 'red' and 'green' channels were displayed graphically. Pearson's correlation coefficients for of transects were calculated and the R^2 values were displayed. Displayed are representatives of these lines, which were drawn randomly at three locations per image.

Table 1. Subtypes of avian influenza virus from which the PB1-F2 proteins were extracted for study

Virus short name	Viral strain	Length of PB1-F2 protein (aa)
H3N8a	A/mallard/Alb/156/2001	90
H3N8b	A/duck/Italy/3139/V06	90
H5N1 5092	A/Turkey/England/5092/91	90
H6N2	A/duck/Italy/2253/V06	90
H8N4	A/mallard/Alb/194/92	90
H9N2 UDL01	A/chicken/Pakistan/UDL01/08	90
H10N7	A/duck/Italy/1398/V06	90
H11N9	A/duck/Italy/6103/V07	90

RESULTS

PB1-F2 proteins from different strains of avian influenza virus have distinct cellular localizations in chicken cells

We analysed the association with mitochondria of PB1-F2, from a wide panel of different avian influenza virus subtypes (Table 1), in a chicken fibroblast cell line (Fig. 1). DF1 cells were transfected with plasmids encoding PB1-F2 proteins with an N-terminal V5 tag and immune-stained for the V5 tag along with Mitotracker dye to highlight the mitochondria before imaging by confocal microscopy. Co-localization between mitochondria and PB1-F2 was quantified by drawing transects through the mitochondria and determining the correlation of pixel intensity for PB1-F2 and mitochondrial staining using Pearson's coefficient. Both visually and by quantification, the PB1-F2 proteins could be categorized into two groups; those with strong mitochondrial co-localization, with Pearson's coefficients of >0.7 (H5N1 50–92, H3N8a and H10N7), and those that showed a diffuse cytoplasmic localization with a weak mitochondria association, with Pearson's coefficients of <0.7 (H9N2 UDL01, H8N4, H11N9, H3N8b and H6N2).

Localization of PB1-F2 in the cytoplasm is determined by amino acids in the C-terminus of the protein

The PB1-F2 proteins of the viruses H9N2 UDL01 and H5N1 50–92 are examples that fell into the two different localization patterns. H9N2 UDL01, R^2=0.243 [±0.032 standard error of the mean SEM)], is predominantly cytoplasmic, whereas H5N1 50–92, R^2=0.749 (±0.024 SEM), is predominantly mitochondria-associated (Figs 1 and 2b). A comparison of the primary amino acid sequences of H9N2 UDL01 and H5N1 50–92 PB1-F2 proteins revealed that there were 11 amino acid differences between them, 4 in the N-terminal region (aa 1–35) and seven in the C-terminus (aa 41–90) (Fig. 2a). Previous reports have demonstrated that the association of PB1-F2 with mitochondria in mammalian cells is determined by the PB1-F2 C-terminus [14, 22, 23]. Therefore we generated chimeric PB1-F2 proteins, whereby a swap of the C-terminus (aa 41–90) was made. We generated UDL01 : 5092 PB1-F2, which contained the N-terminus of H9N2 UDL01 and the C-terminus of H5N1 50–92, and the reciprocal swap 5092:UDL01 PB1-F2 (Fig. 2a). Transects drawn through mitochondria on confocal microscopy images confirmed that V5-PB1-F2 localization to the cytoplasm was determined by the C-terminus of the UDL01 PB1-F2 protein (Fig. 2b). However, the H5N1 5092 C-terminus (UDL01 : 5092) did not enable localization at the mitochondria to the same extent as the H5N1 5092 WT PB1-F2. The UDL01 : 5092 PB1-F2 protein was, however, more efficiently targeted to the mitochondria, with a mean R^2 correlation value of 0.648 (±0.026 SEM), than 5092:UDL01, which was predominantly cytoplasmic, with the mean R^2 correlation value with mitochondria being 0.273 (±0.045 SEM) (Fig. 2b). Previous publications have demonstrated that putative mitochondrial targeting sequences lie between amino acid residues 46 and 75. There were four residues that were different between our two prototypic strains in this aa 46–75 region, so we generated expression constructs that swapped all four mutations in both the H9N2 UDL01 and H5N1 5092 PB1-F2 proteins to analyse in greater detail those residues that contribute to PB1-F2 localization away from the mitochondria. Site-directed mutagenesis at aa 60, 62, 66 and 68 (from R, H, N and I respectively) in H9N2 UDL01 to Q, L, S and T, as is the sequence in H5N1 5092, generated the UDL01-4M PB1-F2 and the reverse mutations in H5N1 5092 generated the 5092–4M PB1-F2. Co-localization of UDL01-4M and 5092–4M PB1-F2 proteins that were V5-tagged with mitochondria via co-staining with Mitotraker Red in DF-1 cells demonstrated that the 5092–4M PB1-F2 was relocalized in a diffuse pattern to the cytoplasm (R^2=0.399) (Fig. 2c), similarly to UDL WT [R^2=0.024 (±0.032 SEM)] and 5092:UDL01 [R^2 =0.273 (±0.045 SEM)]. Conversely, UDL01-4M PB1-F2 had no effect on mitochondrial localization (R^2=0.265) (Fig. 2c), maintaining a similar diffuse cytoplasmic localization to H9N2 UDL, in contrast to the UDL01 : 5092 mutant [R^2=0.647 (±0.045 SEM)]. This suggests that mitochondrial targeting is more easily disrupted than the retargeting of PB1-F2 to the mitochondria, which may require features in the full-length protein. Sequence analysis of the region between aa 46–75 of the other avian influenza virus PB1-F2 proteins from Fig. 1 indicated that the four amino acids identified as being important for the cytoplasmic localization of the H5N1 5092–4M PB1-F2 are not common in cytoplasmic-targeted PB1-F2s. Indeed, the PB1-F2 protein from H8N4 A/Mallard/Alberta/192/92 had a cytoplasmic localization and shared identical residues at these four positions with H5N1 5092, which was mitochondrial-targeted. None of the other PB1-F2 proteins

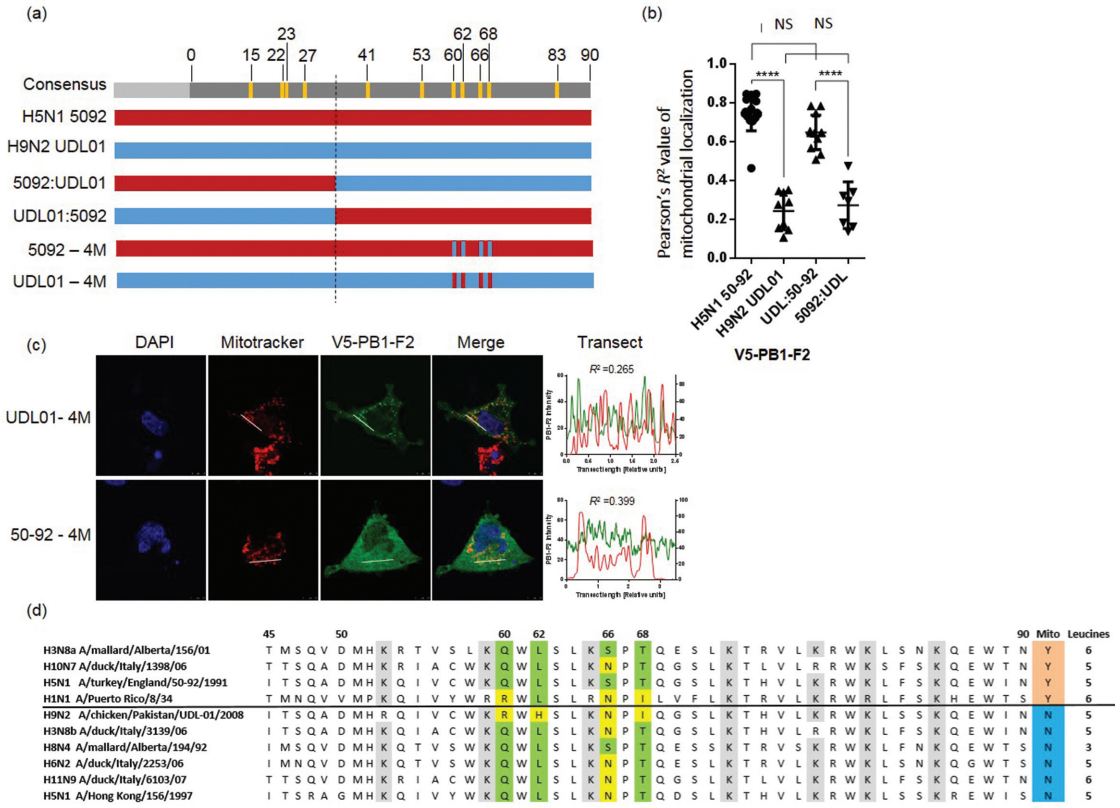

Fig. 2. PB1-F2 protein localization to the mitochondria in chicken cells was mapped to residues in the C-terminus of PB1-F2. (a) Schematic of the amino acid differences between H5N1 5092 (red) and H9N2 UDL01 (blue) PB1-F2 proteins. Chimeric proteins were constructed that had the entire C-terminal portions (5092:UDL01 and UDL01 : 5092) or four residues (60, 62, 66 and 68; 5092–4M and UDL01-4M) swapped between the H5N1 5092 and H9N2 UDL01 strains. (b) and (c) DF-1 cells were transfected with the wild-type V5-PB1-F2 proteins or the V5-PB1-F2 chimeras and stained to indicate the co-localization between V5-PB1-F2 (green) and mitochondria (red). Nuclear staining is indicated by DAPI staining (blue). Transects (white lines) drawn in both the mitochondria and PB1-F2 channel were compared via Pearson's correlation coefficient. In (b) the Pearson's correlation coefficient (R^2) values from 10 cells for each PB1-F2 construct were averaged and plotted. One-way analysis of variance (ANOVA) was used to determine whether significant differences in the correlations existed. ****, P<0.0005; NS, not significant. (d) The C-terminal sequences (aa 45–90) of the PB1-F2 proteins analysed in Fig. 1, in addition to the well-characterized H1N1 (A/PR/8/34) and H5N1 (A/HK/196/97), were aligned. Differences at the 4M mutations (aa 60, 62, 66 and 68) are highlighted, as is mitochondrial localization (mitochondrial=Y, cytoplasmic=N) and the number of leucine residues in the C-terminal fragment (leucines).

shared the 60R, 62 h, 66 N, 68I motif seen in H9N2 UDL01, although the mitochondrial-located PR8 PB1-F2 has 60R, 66 N, 68I (Fig. 2d).

PB1-F2 suppresses interferon-stimulated gene transcripts upon avian influenza virus infection in chicken cells

To provide robust data on the functionality of PB1-F2 to antagonize the type I interferon signalling pathway in chickens we used several different methods. Firstly, we analysed and compared the transcript levels of ISGs in nasal tissue taken from chickens at 2 and 5 days post-infection with isogenic H9N2 viruses that contain the coding capacity for either a full-length PB1-F2 protein (H9N2 UDL01) or a truncation to the initial 11 aa of PB1-F2 (H9N2 UDL01-KO), deemed to be non-functional and therefore a knock-out (Fig. 3a). These two viruses had previously been reported on in James *et al.* and replicated in chicken tissues to similar levels on day 2 post-infection but with the PB1-F2 knock-out H9N2 infectious virus being cleared more quickly on day 5 than the H9N2 with a full-length PB1-F2 protein (Fig. S1) [6]. We observed significantly increased transcript levels for several ISGs and cytokines in the nasal tissue from birds infected by the H9N2 PB1-F2 knock-out virus on both day 2 (Mx, OAS, STAT-1 and IL-6) and day 5 (Mx, IL-6 and IL-1b) post-infection (Fig. 3a).

We utilized primary chicken embryonic fibroblast (CEF) cells and chicken bone marrow-derived monocyte (BMDM) cells to see whether the same upregulation of ISG and cytokine transcripts was observed *in vitro* by avian influenza viruses lacking a functional PB1-F2 protein compared to

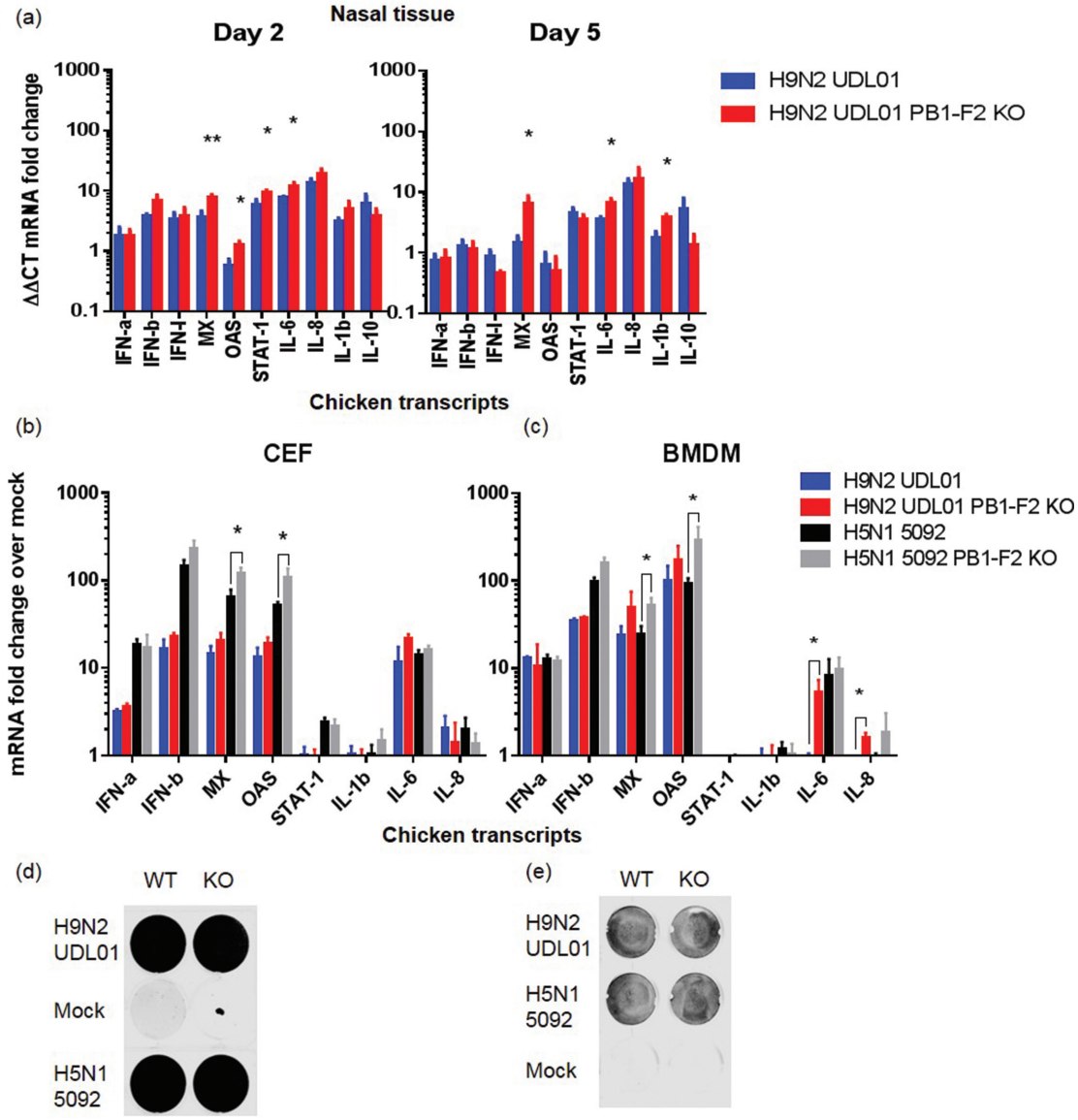

Fig. 3. *In vivo* and *in vitro*, PB1-F2 suppresses chicken interferon-stimulated gene and pro-inflammatory gene transcripts. Total RNA was isolated from the chicken substrates detailed. The RNA was reverse transcribed and used to quantify chicken host response genes via qPCR. Ct values were compared to those of the reference gene RPLP01 and quantified using the ΔΔCt method of quantification. The means +/−SD are shown. Multiple Student's *t*-tests were performed to compare between wild-type and knock-out means and the Holm–Sidak correction for multiple comparisons was applied. *, $P \leq 0.05$; **, $P \leq 0.01$. (a) Nasal tissue taken from six chickens infected with influenza virus possessing a full-length PB1-F2 protein (H9N2 UDL01) or a point mutation abrogating PB1-F2 expression (H9N2 UDL01 KO) at day 2 or day 5 post-infection. (b) Primary chicken embryonic fibroblast (CEF) cells or (c) chicken bone marrow-derived macrophage (BMDM) cells infected with a multiplicity of infection (m.o.i.) of 3 of H9N2 UDL01 or H5N1 5092 viruses that have a full-length PB1-F2 or a knock-out PB1-F2 (KO). At 8 h post-infection, cells were lysedfor RNA isolation, this was repeated in three independent experiments. Supernatants from CEF cells (d) or from chicken BMDM cells (e) infected with H9N2 UDL01 or H5N1 5092 viruses that had a full-length PB1-F2 or a knock-out PB1-F2 (KO) were incubated on Madin–Darby canine kidney (MDCK) cells for 12 h and assayed for the presence of IAV nucleoprotein (NP) with a mouse anti-NP antibody and anti-mouse IRDye 800CW antibody (LI-COR) before being visualized by the Odyssey Imaging System (LI-COR).

those possessing a full-length PB1-F2 protein (Fig. 3b, c). In both cell types, the H5N1 5092 virus pair (H5N1 5092 and H5N1 5092-KO) showed a significant increase in Mx and OAS transcript levels when PB1-F2 was absent during infection and the trend was evident for the H9N2 UDL01 virus pair, although it was not statistically significant. In the BMDM, the transcript levels for IL-6 and IL-8 were significantly elevated when PB1-F2 was absent in the H9N2

UDL01-KO virus and again this trend was evident for the H5N1 5092 virus pair, but it was not statistically significant. The H9N2 UDL01 and H5N1 5092 virus pairs were equally able to infect both CEFs and BMDMs at a multiplicity of infection (m.o.i.) of 3 (Fig. 3d, e). The growth curves of the virus pairs in primary chicken kidney cells (Fig. S4a) showed that for both pairs of viruses there was no difference in infectious virus release at early time points post-infection, up to 24 h. We did observe significantly more virus at 48 h post-infection in the growth curve for the H5N1 5092 PB1-F2 KO virus compared to H5N1 5092 WT. In the chicken fibroblast DF-1 cell line, the reconstituted viral polymerase activity of both the H5N1 5092 and H9N2 UDL01 viruses was not affected by the ability of the PB1 segment to encode a full-length PB1-F2 (Fig. S4b). Our *in vitro* infections suggested that the PB1-F2 of both H9N2 UDL01 and H5N1 5092 was able to suppress ISG and pro-inflammation cytokines transcripts, but the potency of the antagonism varied. There was a trend in the *in vitro*-tested substrates, CEFs and chicken BMDM for the PB1-F2 of H5N1 5092 to be able to antagonize chicken IFN1- and IFN2-stimulated genes, Mx and OAS more potently upon infection (a difference of 50–250-fold compared to H5N1 5092-KO), whereas the H9N2 UDL01 PB1-F2 displayed a more modest 20-fold difference compared with H9N2 UDL01-KO. In contrast, the H9N2 UDL01 PB1-F2 antagonized the pro-inflammation cytokines IL-6 and IL-8 more potently than H5N1 5092 PB1-F2 upon infection (Fig. S3 b-c).

Co-localization with the mitochondria and consequently MAVS enhances chicken IFN-2 promoter antagonism by PB1-F2

We performed a co-localization study in chicken DF-1 cells by overexpression of a V5-tagged chicken MAVS construct (ckMAVS-V5) and a FLAG-tagged version of the H9N2 UDL01 and H5N1 5092 PB1-F2 proteins (Figs 4a and S2). Similarly to the co-localization with Mitotraker, we performed immune staining against the FLAG and V5 tags and drew transect lines through the confocal images along the ckMAVS-V5 staining and the correlation of pixel intensity along these transects for each stain was then calculated using Pearson's coefficient. We observed that mitochondrial-targeted H5N1 5092 PB1-F2 protein had a strong co-localization with ckMAVS (R^2=0.851±0.022 SEM), whereas the H9N2 UDL01 PB1-F2 protein only had a weak correlation (R^2=0.332±0.042 SEM); a GFP-FLAG expression construct was used as a control and showed no co-localization with ckMAVS-V5 (R^2=−0.002±0.020 SEM) (Fig. 4a). Co-immunoprecipitation using an anti-V5 antibody from DF-1 cells expressing ckMAVS-V5 and either FLAG-tagged H5N1 5092 or H9N2 UDL01 PB1-F2 demonstrated that both PB1-F2 proteins could interact with ckMAVS, but that the efficiency of the binding differed, with the H5N1 5092 PB1-F2 associating to a greater extent with ckMAVS than H9N2 UDL01 (Fig. 4b).

Having already detailed the cellular localization difference of the PB1-F2 proteins, H9N2 UDL01 and H5N1 5092, we hypothesized that cellular localization could influence the potency with which type 1 IFN was induced and consequently ISGs during infection. Therefore we used a well-described IFN bioassay that makes use of type 1 IFN inhibition of a GFP vesicular stomatitis virus (VSV-GFP) to determine the ability of the PB1-F2 proteins to antagonize the production of bioactive chicken IFN from DF-1 chicken cells [26]. We applied equal volumes of virus-inactivated supernatant taken from chicken BMDM cells infected with H9N2 UDL01 and H5N1 5092 isogenic virus pairs that contained a full-length PB1-F2 or PB1-F2 KO, at a high m.o.i. to DF-1 cells, as a primer, prior to infection of the DF-1s by VSV-GFP. The level of GFP fluorescence measured in the cells was therefore inversely proportional to the relative levels of IFNs secreted during the initial influenza infection. We found that in both virus pairs the parental viruses that contained a full-length PB1-F2 protein induced less type 1 IFN following infection than the viruses that were knocked out for PB1-F2 (Fig. 4c). This suggested that the level of IFN induction was suppressed more by the PB1-F2 from H5N1 5092, which is located predominantly at the mitochondria, co-localized with ckMAVS, than the PB1-F2 from H9N2 UDL01, which has a more modest co-localization with MAVS and a predominantly cytoplasmic cellular localization.

To increase the clarity of the relationship between subcellular localization of PB1-F2 and the antagonism of IFN and the subsequently induced ISGs, we utilized a chicken IFN-2 promoter firefly luciferase reporter construct in DF-1 cells. The reporter was co-transfected with poly I : C, which can induce the IFN- 2 promoter, a constitutively expressed *Renilla* reporter and PB1-F2 plasmids. We compared the ability of H5N1 5092 PB1-F2 with that of H9N2 UDL01 PB1-F2 and found that, in line with our other results, H5N1 5092 PB1-F2 was more potent in the antagonism of the chicken IFN- 2 promoter (Fig. 4d). In conjunction, we utilized the chimeric PB1-F2 proteins containing the reciprocal C-terminus swaps, 5092:UDL01 and UDL01 : 5092, which show altered cellular localizations with respect to the mitochondria, compared to the parental PB1-F2 proteins. Our results demonstrated that possession of the H9N2 UDL01 C-terminus, which disrupted mitochondrial localization, resulted in a reduced antagonism of the chicken IFN-2 promoter compared to those PB1-F2 proteins containing the H5N1 5092 C-terminus (Fig. 4d).

Co-localization with the mitochondria did not correlate with enhanced PB1-F2 antagonism of an NFκB responsive promoter

Influenza virus infection is known to activate NFκB transcription of cytokines involved in inflammation, such as IL-8 and IL-1b. In chickens infected by a H9N2 virus that possessed a full-length PB1-F2 protein, some of the transcripts for pro-inflammatory genes, e.g. IL-6 and IL-1b, were supressed compared to infection where the PB1-F2 was absent (Fig. 3a). To determine whether PB1-F2 from the avian influenza strains H9N2 UDL01 and H5N1 5092

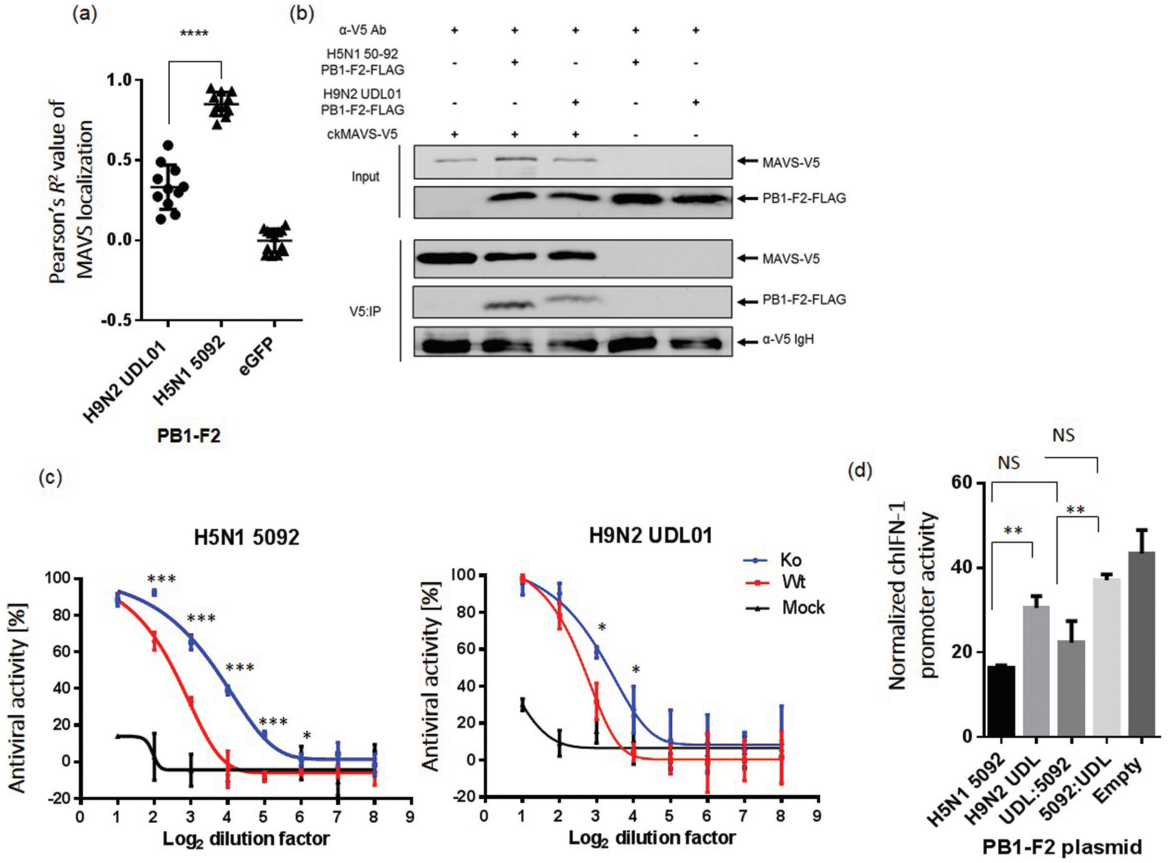

Fig. 4. Co-localization of PB1-F2 with mitochondria increases the antagonism of the IFN2 promoter. (a) DF-1 cells were transfected with over-expression plasmids for the wild-type FLAG-tagged PB1-F2 proteins or eGFP and chicken MAVS-V5. Transects were drawn in both the MAVS and PB1-F2/eGFP channel and co-localization via pixel intensity was compared using Pearson's correlation coefficient. Pearson's correlation coefficient (R^2) values from 10 cells for each PB1-F2 construct and eGFP were averaged and plotted. One-way ANOVA was used to determine whether significant differences in the correlations existed. ****, P<0.0005. (b) DF1 cells were co-transfected with PB1-F2-FLAG and chicken MAVS–V5 expression constructs in varying combinations, as shown. The input expression levels of PB1-F2 and ckMAVS plus the resultant co-immunoprecipitation pulled down proteins on protein G beads by an anti-V5 antibody. This image is representative of the experiment, which was performed twice. (c) UV-inactivated cell supernatants from high-m.o.i. influenza virus infections of BMDMs were serially diluted ($\log_2$) and incubated on DF-1 cells for 12 h. Cells were washed and incubated with VSV-GFP virus for 12 h and fluorescence was read at 560 nm. The means +/−SD are shown. This data are representative of at least two independent repeats. Viruses were isogenic pairs of H5N1 5092 and H9N2 UDL01 with point mutation to knock out functional full-length PB1-F2 protein (K), blue) or wild-type PB1-F2 coding capacity (WT, red). Mock samples were uninfected cell supernatants. (d) DF-1 cells were transfected with a chicken IFN-2 promoter firefly luciferase reporter, constitutively active *Renilla* expression plasmid and 2 µg of PB1-F2 overexpression plasmid. Twelve hours post-transfection, cells were re-transfected with 0.25 µg of poly I : C . At 24 h post-transfection, cells were lysed and luciferase activity was quantified. The luciferase intensities were normalized to *Renilla* expression. The means of three independent experiments +/−SD and one-way ANOVA analysis was performed. **, P<0.005; NS, not significant.

specifically antagonized NFκB activation, we utilized a NFκB response element luciferase reporter construct in chicken DF-1 cells, and this was co-transfected with a constitutively active *Renilla* luciferase plasmid and PB1-F2 plasmids. Cells were stimulated by transfection with poly (poly I : C), which activated NFκB, leading to luciferase induction. Co-expression of H9N2 UDL01 PB1-F2 significantly inhibited the luciferase signal, whereas co-expression of H5N1 5092 PB1-F2 did not, although there was a trend in multiple assays for the luciferase signal to be lower than for no PB1-F2 expression (empty) (Fig. 5a). H9N2 UDL01 PB1-F2 inhibition of the NFκB response element was due to the inhibition of NFκB nuclear translocation (Fig. S3).

We utilized our C-terminus-swapped PB1-F2 constructs to determine the contribution of the C-terminus sequence, and by inference cellular localization, to the ability of PB1-F2 to antagonize NFκB activity. We found that both 5092:UDL01 and UDL01 : 5092 PB1-F2 proteins were able to significantly inhibit NFκB-responsive promoter activity in this set-up (Fig. 5a). UDL01 : 5092 was only partially mitochondrial-

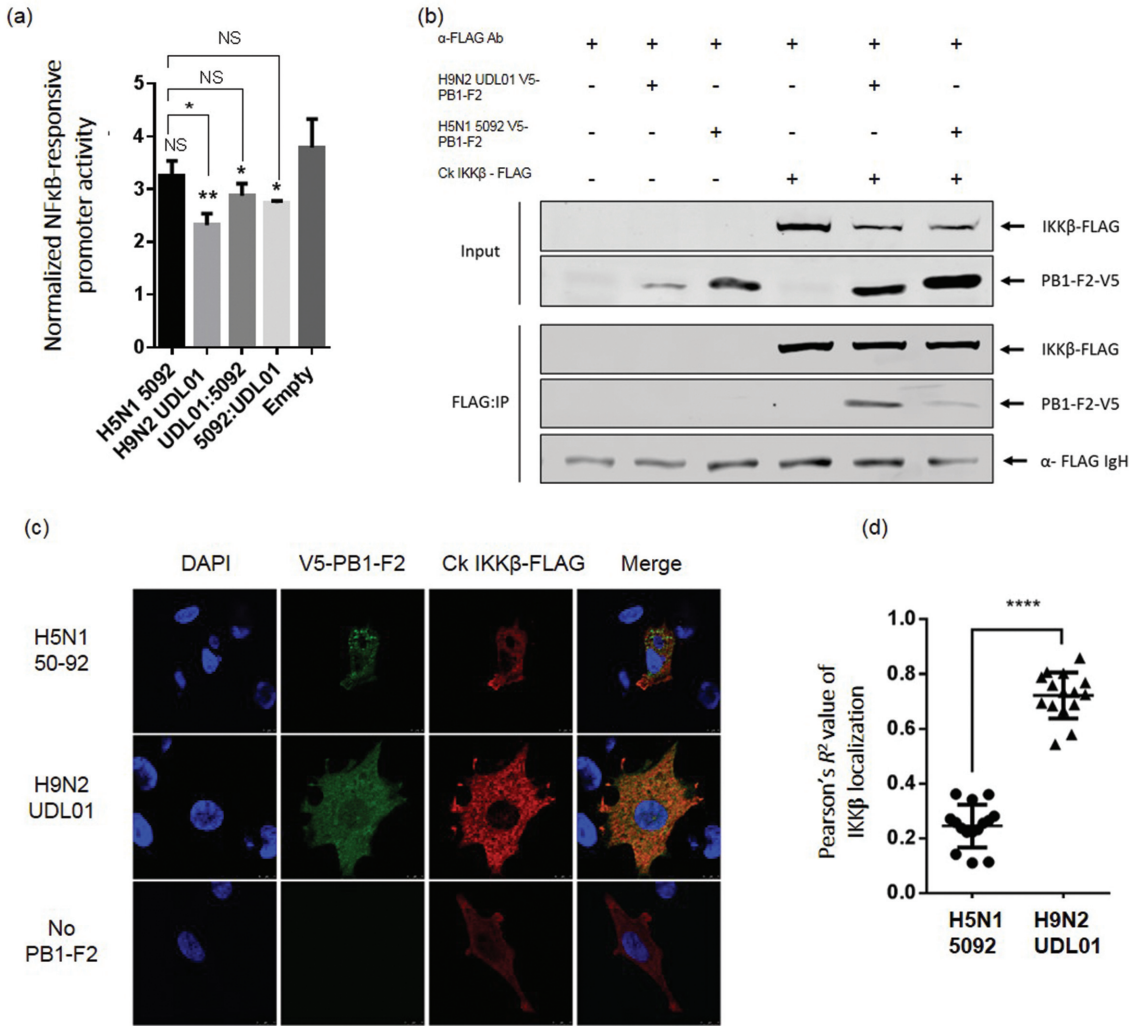

Fig. 5. Co-localization of PB1-F2 with the mitochondria reduced interaction with IKKβ and antagonism of NFκB activity. (a) DF-1 cells were transfected with an NFκB-dependent promoter firefly luciferase reporter, constitutively active *Renilla* expression plasmid and 2 µg V5-PB1-F2 overexpression plasmid. 12 h post-transfection cells were stimulated with poly I : C. At 24 h post-transfection cells were lysed and luciferase activity was quantified. The luciferase intensities were normalized to *Renilla* expression. The means of three independent experiments +/− SD and one-way ANOVA analysis was performed. **, P<0.005; NS, not significant. (b) DF1 cells were co-transfected with V5-PB1-F2 and chicken IKKβ-FLAG expression constructs in varying combinations, as shown. The input expression levels of V5-PB1-F2 and ckIKKβ-FLAG plus the resultant co-immunoprecipitation pulled-down proteins on protein G beads by an anti-FLAG antibody. This image is representative of the experiment, which was performed twice. (c) DF-1 cells were transfected with combinations of ckIKK-β-Flag and V5-PB1-F2 expression plasmids. Twelve hours post-transfection cells were fixed and immunostained with antibodies against FLAG [ckIKK-β (red)] and V5 [PB1-F2 (green)] and stained with DAPI [nucleus (blue)]. (d) Pearson's correlation coefficients of ckIKK-β-Flag and V5-PB1-F2 co-localization were calculated. This was performed for at least 15 separate images from 2 independent experiments and displayed graphically. Significance was calculated using Student's t-test ****, $P\leq$0.0001.

localized compared to H5N1 5092, which may explain this result.

Cytosolic localization of PB1-F2 provides increased opportunity to directly interact with IKKβ but reduces PB1-F2 cellular stability

We tested the ability of H5N1 5092 and H9N2 UDL01 PB1-F2 to interact with chicken IKKβ using co-immunoprecipitation in DF-1 cells (Fig. 5b). Both V5-tagged H9N2 UDL01 and H5N1 5092 PB1-F2 proteins were shown to co-precipitate with a FLAG-tagged chicken IKKβ. The pulldown was more efficient with H9N2 UDL01 PB1-F2 than with H5N1 5092 PB1-F2, despite less H9N2 UDL01 PB1-F2 protein being present in the input samples (Fig. 5b). We also saw that in DF-1 cells chicken IKKβ localized more closely with the PB1-F2 of H9N2 UDL01 than that of H5N1 5092 (Fig. 5c, d). A general feature of our work with the

H9N2 PB1-F2 protein was the instability of the protein in cells; we required the use of MG132, a well-described proteasome inhibitor in order to obtain good visualization in cells and by Western blot. Despite the PB1-F2 proteins being cloned into the same plasmid background, with identical promoters and Kozak sequences, the H5N1 5092 PB1-F2 protein does not have the same instability seen with H9N2 UDL01 PB1-F2 (Fig. 6a). We hypothesized that the difference in cellular location of the two PB1-F2 proteins may result in different exposure to proteasomal-mediated degradation, with interaction with MAVS at the mitochondria somehow shielding the H5N1 5092 PB1-F2 from degradation. To provide a quantified measure of protein stability in chicken DF-1 cells, we performed a cycloheximide chase assay and levels of PB1-F2 expression were determined post-application of cycloheximide by Western blot. The H9N2 UDL01 PB1-F2 degrades significantly from the levels detected at the point of cycloheximide application (time=0) within 30 min, whereas by 8 h post-cycloheximide application, the H5N1 5092 PB1-F2 is still visible (Fig. 6a-c).

In Fig. 2 we demonstrated that swapping the H5N1 5092 C-terminus (5092:UDL01), or the four amino acids termed '4M', for those in the H9N2 UDL01 (5092–4M) resulted in a disruption of the mitochondrial localization of H5N1 5092, although the reciprocal mutations swaps did not completely relocalize H9N2 UDL01 PB1-F2 from the diffuse cytoplasmic staining pattern to the equivalent level of H5N1 5092. We used the panel of mutant PB1-F2 proteins in the cycloheximide chase assay and looked at the time point 1 h after the addition of cycloheximide to transfected DF-1 cells. We found that disrupting the mitochondrial localization (5092:UDL01 and 5092–4M) resulted in a significant difference in the stability of the PB1-F2 proteins (Fig. 6b, c).

DISCUSSION

The capacity of IAV to encode a full-length PB1-F2 is conserved in 93 % of all avian host-isolated IAVs, compared to 43 and 48 % from human and swine host isolates. We have previously demonstrated that the presence of a full-length PB1-F2 in an avian IAV resulted in a longer virus shedding profile in chickens and increased viral tissue dissemination in infected birds, and that these outcomes had a cumulative effect of prolonging the transmission window of the virus from an infected chicken to a naïve sentinel chicken [6]. The absence of a full-length PB1-F2 also resulted in an increase in viral pathogenicity in chickens in both our previous study and that by Leymaire *et al.* (2014) [6, 11]. PB1-F2 has been described previously to have cell-type-specific and viral strain-specific activities. Here we show that PB1-F2 proteins from two avian IAVs of the subtypes H5N1 and H9N2 inhibit the production of type I IFN in chicken cells and can interact with chicken MAVS upstream of the type 1 interferon promoter (Figs 3 and 4). In addition, these two PB1-F2 proteins can antagonize NFκB activation and interact with chicken IKKβ (Fig. 5). PB1-F2-induced suppression of type 1 IFN and NFκB must occur *in vivo* in chickens, since lower levels of ISG and pro-inflammation transcripts, which are stimulated by onward signalling from type 1 IFN induction and NFκB activation, were observed in nasal tissue from birds that were infected by H9N2 IAV containing an intact PB1-F2 protein. Specifically, the abundance of transcripts for the ISGs MX, OAS and STAT-1 and the pro-inflammatory-associated cytokines IL-6 and IL-1β were all significantly reduced when infection was by a virus possessing a full-length PB1-F2 protein as compared to infection by an isogenic virus that did not encode a functional PB1-F2. This suppression of ISGs and pro-inflammation signals was also observed in a PB1-F2-dependent manner *in vitro* in primary chicken fibroblasts and macrophages. Some differences in the magnitudes of the transcript levels were observed between the CEFs and chicken BMDM upon infection by isogenic viruses that differed only by the presence of PB1-F2, but this was likely due to different sensitivities of fibroblast and myeloid cells to these induction signals, since the entry by the viruses at high m.o.i. appeared to be equal. There was little difference in the magnitude of apoptosis caused by the individual viruses in the two different cell lines as measured using a capsase3/7 activity reporter (data not shown). Leymarie *et al.* also report for another H5N1 influenza isolate that the presence of PB1-F2 suppresses innate responsive transcripts during chicken infection [11].

There are clear differences in the components of the type 1 interferon pathway between mammals and chickens, such as the lack of the pattern recognition receptor (PRR) RIG-I and transcription factor IRF-3 in chickens. Instead, the influenza pathogen-associated molecular pattern is recognized by the 'RIG-I like receptor' MDA5 in chicken cells, which then signals via chicken MAVS located at the mitochondria to the transcription factor IRF-7, which induces the type 1 interferon promoter in the nucleus [27]. In this study we have demonstrated for the first time an interaction between chicken MAVS, the mitochondrial-located interferon induction pathway adapter and PB1-F2 of two avian IAV strains. The interaction of PB1-F2 with human MAVs has been demonstrated, previously, but there is only 39 % homology at the amino acid level between chicken and human MAVS [19]. Our co-immunoprecipitation results suggested that the interaction with chicken MAVS was more efficient with the PB1-F2 from H5N1 5092 as compared to H9N2 UDL01, although both did display the interaction. In human 293T cells, Varga *et al.* showed that PB1-F2 of the vaccine strain A/PR/8/34 interacted with MAVS at the mitochondria and this resulted in a decreased mitochondrial membrane potential and antagonism of type 1 interferon production [19, 20]. It is likely that a similar mechanism is the cause of the type 1 interferon induction antagonism seen in chicken cells by PB1-F2,

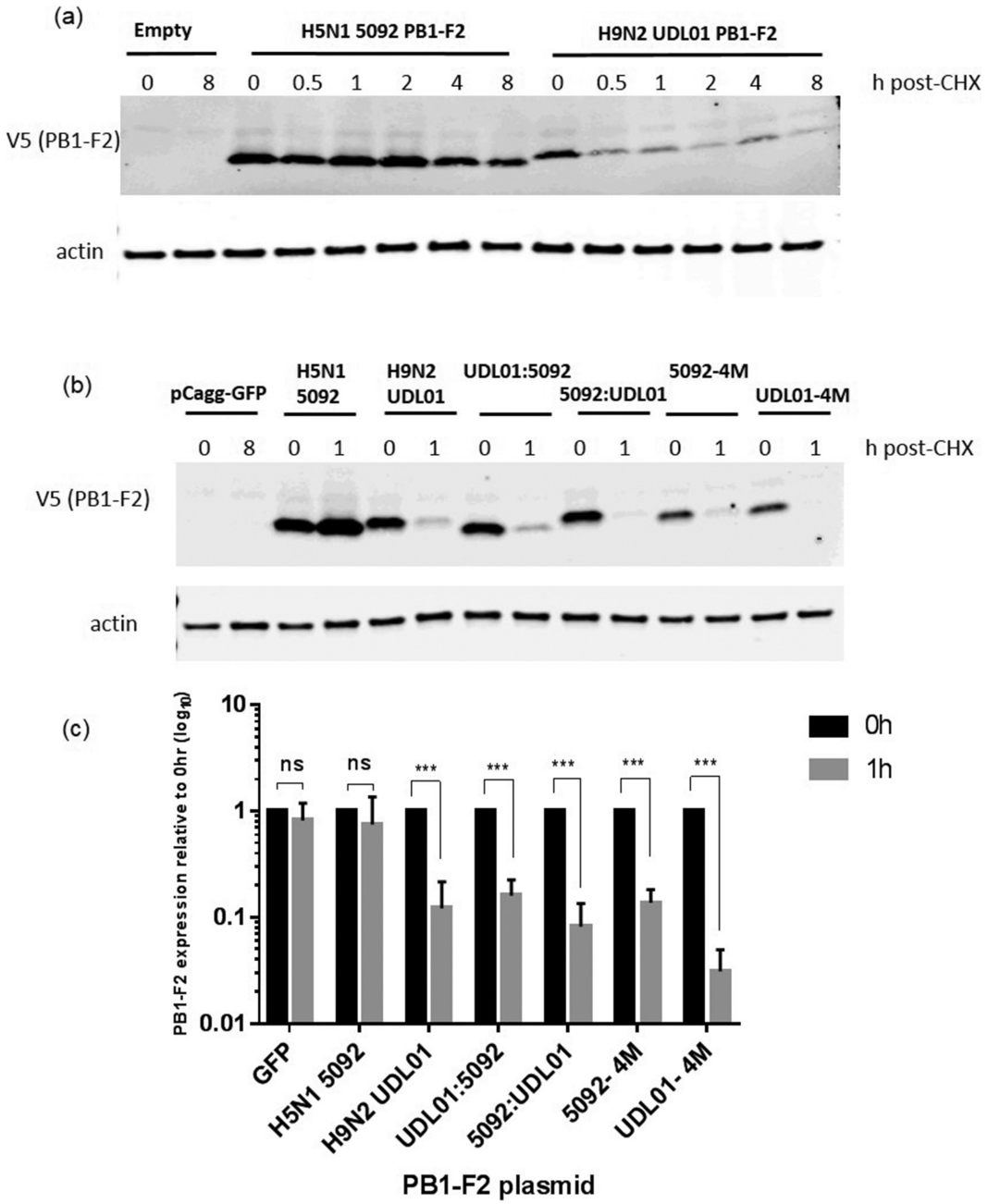

Fig. 6. Stability of PB1-F2 protein in chicken cells. (a) DF-1 cells were transfected with expression plasmids for H9N2 UDL01 and H5N1 5092 PB1-F2 V5 tagged proteins. At 24 h post-transfection cycloheximide was applied to the cells and then the cells were lysed at various time points, as indicated. Lysates were run on western blot and probed for V5 (PB1-F2) and actin as a loading control. (b) A cycloheximide chase assay was performed on DF-1 cells transfected with various wild-type, C-terminal swap and 4M PB1-F2 mutants, as indicated. The levels of V5-PB1-F2 at time of cycloheximide addition (0 h) and after 1 h were probed using anti-V5 antibody and actin as a loading control. (c) Densitometry was performed on the V5-PB1-F2 band of the cycloheximide chase assay for both 0 and 1 h time points. Signal was normalized for actin and 0 h for each V5-PB1-F2 construct was set to 1. Relative V5- PB1-F2 levels at 1 h post-cycloheximide addition were calculated and are represented graphically. The average of three independent repeats is displayed and the standard deviation is indicated by error bars. Significance were calculated using Student's *t*-test. ***, $P \leq 0.0005$; ns, not significant.

since we can demonstrate that interaction does occur with chicken MAVS and that greater antagonism is seen by PB1-F2 proteins that co-localize at the mitochondria with MAVS, e.g. the H5N1 5092 PB1-F2 protein compared to the H9N2 UDL01 PB1-F2 (Figs 1, 2 and S3).

Additionally, we have demonstrated interaction between PB1-F2 and chicken IKKβ for the first time. When NFκB is released from inhibition it translocates into the nucleus and acts as a transcription factor stimulating the transcription of innate response genes, and the phosphorylation action of the serine kinase, IKKβ, on Iκb releases NFκB inhibition. It has been shown previously that PB1-F2 is able to interact directly with human IKKβ [28]. There is an 83 % amino acid conservation between human and the chicken IKKβ homologue. We found that the H9N2 UDL01 PB1-F2 had a more efficient interaction with IKKβ than H5N1 5092. We hypothesize that interaction with chicken MAVS results in the inhibition of onward interferon induction pathway simulation and is likely how PB1-F2 elicits an effect on ISG levels, and similarly, the interaction of PB1-F2 with IKKβ may prevent the phosphorylation of Iκb and thus inhibit the translocation of NFκB to the nucleus, resulting in the inhibition of pro-inflammation cytokines. The variability in the strength of the interaction of the avian influenza virus PB1-F2 proteins with either chicken MAVS or chicken IKKβ corresponded to the potency of the two PB1-F2 proteins to antagonize type I IFN induction and NFκB activation. More H5N1 5092 PB1-F2 was precipitated with chicken MAVS and it also had a greater ability to antagonize the type I IFN induction pathway as compared to H9N2 UDL01 PB1-F2. In contrast, H9N2 UDL01 PB1-F2 had a more substantial interaction with IKKβ and was able to antagonize the activation of an NFκB dependent promoter significantly in comparison to the H5N1 5092 PB1-F2 protein. The differences in antagonism potency correlated with the degree of PB1-F2 localization to the mitochondria. Significant co-localization with mitochondrial markers, including MAVS, was associated with enhanced antagonism of type I IFN production, but reduced NFκB activation inhibition. Taken together, this work suggests a mechanism by which PB1-F2 can interact with chicken MAVS and chicken IKK-β to downregulate type 1 IFN and the downstream pro-inflammatory signals in infected cells *in vivo*, which results in reduced pathogenicity and impaired viral clearance in chickens.

Cellular localization was established for a panel of avian influenza PB1-F2 proteins, which clearly established two phenotypes: predominantly mitochondrial or predominantly cytoplasmic (Fig. 1). The two PB1-F2 proteins investigated here, H5N1 5092 and H9N2 UDL01, were representative of each group, with H5N1 5092 being preferentially localized to the mitochondria, the location of chicken MAVS (Fig. S2), and H9N2 UDL01 having a diffuse cytoplasmic localization that was the same as chicken IKKβ (Fig. 5 c). It has previously been demonstrated that the C-terminus is responsible for the mitochondrial localization of PB1-F2 in mammalian cells [23] and indeed when we swapped the C-terminus portions of the H5N1 5092 for that of H9N2 UDL01 PB1-F2 proteins we observed a relocalization away from the mitochondria to the cytoplasm in chicken fibroblast cells (Fig. 2). However, a reciprocal swap only partially retargeted the PB1-F2 to the mitochondria, with statistical analysis by Student' s *t*-test between the Pearson's localization value for H5N1 5092 and UDL01 : 5092 indicating that they were still significantly different (*P* value=0.008). This suggests that features in the N-terminus of the H5N1 5092 PB1-F2 make an additional contribution to mitochondrial localization. By altering only four amino acids in the C-terminus of the H5N1 5092 to those found in the H9N2 UDL01 PB1-F2 protein (Q60R, L62H, S66N and T68I), producing our 5092–4M mutant, we disrupted the H5N1 5092 mitochondrial association (Fig. 2 c). A triple mutant H5N1 5092 PB1-F2 protein (L62H, S66N, T68I) where residues were changed to those found in the H9N2 UDL01 PB1-F2, as in the 5092–4M mutant, did not result in significant retargeting of the H5N1 5092 PB1-F2 (data not shown). Cheng *et al.* showed that the introduction of the motif I68, L69, V70 and F71 to H5N1 A/Hong Kong/156/97 relocated this PB1-F2 to the mitochondria in mammalian cells, while replacement of this motif in the PB1-F2 of H1N1 A/Puerto Rico/8/34 removed mitochondria association [22]. We found no conservation of this motif in the PB1-F2 proteins we analysed for cellular localization. Similarly, Chen *et al.* demonstrated an enhancement of the mitochondrial localization of H5N1 A/Hong Kong/156/97 PB1-F2 when two additional leucine residues (Q69L and H75L) were introduced in the C-terminus [23]. Our analysis shows no correlation between the numbers of leucine residues in the C-terminus of PB1-F2 and whether predominant mitochondrial localization occurs in chicken cells (Fig. 2d). Gibbs *et al.* postulated the presence of an amphipathic helix and a short preceding hydrophobic patch in the C-terminus of PR8 PB1-F2 (aa 65–87) and hypothesized that this was responsible for the targeting of the protein to the mitochondria [24]. We again found no correspondence between this area of sequence; all the sequences we analysed, regardless of observed cellular localization, had a predicted helix structure and four out of the five basic residues observed in the PR8 amphipathic helix. The upstream hydrophobic residue patch was the same between viruses that had different cellular localization.

PB1-F2 has a short half-life within cells and becomes ubiquitinated on conserved lysine residues in the C-terminus as a post-translational modification [10]. Kosik *et al.* demonstrated that mutation of the C-terminal lysine residues at positions 73, 78 and 85 to arginines reduced ubiquitination and increased the stability of PB1-F2 in mammalian cells. We found that H9N2 UDL01 had one fewer lysine residue in the C-terminus sequence compared to H5N1 5092 (Fig. 2d), but when the stability of both the H9N2 UDL01 and the H5N1 5092 PB1-F2 proteins and the derived C-terminal-altered mutants in chicken cells was assessed, we found that cellular localization, not the presence of lysines in the C-terminal sequence, correlated with protein stability. H5N1 5092 had a strong co-localization with the mitochondria and was the PB1-F2 protein that was most stable in chicken DF-1 cells. In contrast, disruption of the H5N1 5092 mitochondrial localization via C-terminal (5092: UDL01) or four-residue swap (5092–4M) with the H9N2

UDL01 PB1-F2 resulted in significant degradation of the PB1-F2 protein by 1 h after the addition of cycloheximide. We suggest, therefore, that PB1-F2 proteins that are predominantly targeted to the mitochondria are protected from ubiquitin-directed proteosomal degradation compared to PB1-F2 proteins that have a diffuse cytoplasmic localization. Indeed, studies by others also support this hypothesis; Cheng *et al.* demonstrate that the predominantly mitochondria-located PB1-F2 of A/Puerto Rico/8/34 has a significantly longer half-life in HeLa cells compared to the PB1-F2 from A/Hong Kong/156/97, which is cytoplasmic in localization, and this finding has also been observed by Kosik *et al.* for the same strains in 293T cells [10, 22]. Chen *et al.* showed that a H1N1 A/Taiwan/3355/1997 PB1-F2 that localized to the mitochondria had the same stability in 293T cells as the A/Puerto Rico/8/34 PB1-F2 [23]. PB1-F2 has been shown to have a dramatically differing secondary structure that is dependent upon the sequence and the environment in which the proteins reside [29, 30]. In aqueous solution, PB1-F2 isdisordered and in the presence of membranes PB!-F2 can form a structured fibre which can disrupt those membranes [8]. The differing predominant localizations of the H5N1 5092 and H9N2 UDL01 PB1-F2 viruses could influence the protein structure in infected cells and consequently their functionality.

Our results suggest that the PB1-F2 protein can operate at different points within innate immune signalling pathways in a strain-specific manner that is reminiscent of the influenza NS-1 protein, and that localization of PB1-F2 in the cell is a driving factor of the protein's functionality. PB1-F2 is encoded from the +1 reading frame of the functionally important RNA-dependent RNA polymerase, PB1. Analyses indicate that the first two positions in the codon of PB1-F2 vary more than position three, which is in line with +1 translation frame from PB1, and this contributes to the high non-synonymous-to-synonymous ratio found for PB1-F2 proteins [31, 32]. The fact that PB1-F2 proteins with different amino acid sequences can use various mechanisms to achieve the same innate pathway antagonism indicates that this function is important, at least in avian cells. Whether evolution of the other viral proteins overrides selection towards one mechanism or another is yet to be determined.

METHODS

Ethics statement

All animal work was approved and regulated by the UK Government Home Office under the project licence PPL 30/2952. All personnel involved in the procedures were licensed by the UK Home Office. Euthanasia of chickens was carried out by intravenous administration of sodium pentobarbital and confirmed through cervical dislocation.

Cells

Madin–Darby canine kidney (MDCK), 293T and chicken fibroblast Doug Foster 1 (DF-1) cells were grown in complete media [DMEM (Gibco-Invitrogen, Inc.)] supplemented with 10 % foetal bovine serum (FBS) (Biosera, Inc.), 1 % penicillin/streptomycin (Sigma-Aldrich) and 1 % non-essential aa (Sigma-Aldrich), and maintained at 37 °C in 5 % CO_2.

Primary chicken embryo fibroblasts (CEFs) were produced from 10-day-old Rhode Island Red chicken embryos from specific-pathogen-free (SPF) hens. Embryos were homogenized and trypsinized with 0.25 % trypsin/EDTA solution (Sigma-Aldrich). The homogenate was resuspended in complete media and passed through a Falcon Cell Strainer (Fisher) before being seeded onto plates for experimentation. Influenza infections were conducted in Eagle's minimum essential medium (EMEM) supplemented with 0.35 % bovine serum albumin (BSA) (Sigma-Aldrich), 1 % penicillin/streptomycin and 0.25 μg ml^{-1} TPCK-treated trypsin.

Primary chicken bone marrow-derived macrophage cells (ckBMDM) were produced from male 3-week-old Rhode Island Red chickens from a SPF flock. Femurs were extracted, and the marrow was flushed and liberated with phosphate-buffered saline (PBS). The cells were homogenized, passed through a Falcon Cell Strainer and then isolated via centrifugation on Histopaque 1083 (Sigma-Aldrich). The cells were washed and resuspended in Roswell Park Memorial Institute medium-1640 (RPMI-1640) medium (Invitrogen) supplemented with 5 % FBS and 5 % chicken serum (Pirbright), 2.95 g l^{-1} TBP (Sigma-Aldrich), 1 mM sodium pyruvate (Sigma-Aldrich) and 1 % penicillin/streptomycin, and seeded onto plates for experimentation. BMDMs were stimulated to differentiate by the addition of 10 ng ml^{-1} of chicken colony-stimulating factor 1 (cCSF-1) for 5 days (The Roslin Institute). Influenza infections were conducted in the same media without serum.

Primary chicken kidney cells (CKCs) were produced from 2–3-week-old Rhode Island Red chickens from a SPF flock. Kidneys were extracted, homogenized and trypsinized with 0.25 % trypsin/EDTA solution (Sigma). The homogenate was washed and resuspended in EMEM (Invitrogen) supplemented with 10 % FBS (Sigma), 2.95 g l^{-1} tryptose phosphate broth (TPB) (Sigma), 10 mM HEPES (Sigma) and 1× penicillin/streptomycin (Sigma). The homogenate was passed through a Falcon Cell Strainer (Fisher) and seeded onto plates for experimentation. Influenza infections were conducted in the same medium without serum.

Viruses

Recombinant A/chicken/Pakistan/UDL01/08 H9N2 virus (H9N2 UDL01) and a reassortant H5N1 5092 influenza virus where the NS, NP, PA, PB1 and PB2 viral genetic segments were from A/Turkey/England/5092/91 H5N1 virus and the HA, NA and M viral genetic segments were from the vaccine strain A/PR/8/34 H1N1 virus, were generated using reverse genetics. Both H9N2 UDL01 PB1-F2-KO and H5N1 5091 PB1-F2-KO viruses were generated by the introduction of a stop codon at aa position 12 in the PB1-F2 reading frame; this was constructed by site-directed mutagenesis in the PB1 genetic segment prior to reverse genetics

rescue of virus. Reverse genetics virus rescue was performed by the transfection of human embryonic kidney (HEK) 293T cells (ATCC) and co-culture in MDCK cells (ATCC) with the addition of 2 μg ml^{-1} of TPCK-treated trypsin (Sigma-Aldrich).

Expression plasmids

The open reading frame (ORF) of PB1-F2 from the listed avian influenza viruses – H5N1 50–92 (A/Turkey/England/5092/91), H3N8a (A/mallard/Alb/156/2001), H10N7 (A/duck/Italy/1398/V06), H9N2 UDL01 (A/chicken/Pakistan/UDL01/08), H8N4 (A/mallard/Alb/194/92), H11N9 (A/duck/Italy/6103/V07), H3N8b (A/duck/Italy/3139/V06) and H6N2 (A/duck/Italy/2253/V06) – were cloned into the eukaryotic expression vector pCAGGs with an N-terminal V5 tag placed in-frame. H5N1 5092 and H9N2 UDL01 PB1-F2 protein were also cloned in the pCAGGs expression vector with an in-frame FLAG tag at the N-terminus. These PB1-F2 expression plasmids, along with a pCAGGs vector containing eGFP, were used in confocal microscopy and co-immunoprecipitation experiments. Full-length cDNA clones of chicken MAVS and chicken IKKβ were generated from DF1 cells treated with chicken IFN (1000 U ml^{-1}) overnight and cloned into the expression plasmid pEF. pLink2 [33].

Co-localization studies in DF-1 cells

DF-1 cells were grown on coverslips before being transfected with the appropriate expression plasmids. Four hours post-transfection, 5 μM MG132 (Sigma-Aldrich) was applied to the cells. At 12 h, post-transfection cells were fixed in 10 % formalin (Sigma-Aldrich) and then permeabilized in 0.1 % Triton X-100 (Sigma-Aldrich) in PBS. For mitochondrial staining, cells were incubated in serum-free DMEM containing 200 nM of MitoTracker CMX-Ros (Thermo Fisher) prior to fixation. Nuclei were stained with 0.2 μg ml^{-1} of DAPI (4′,6-diamidino-2-phenylindole) (Sigma-Aldrich) in dH_2O. Proteins tagged with V5 or FLAG were stained using a 1 : 1000 dilution of either rabbit αV5 (GeneTex), mouse anti-V5 (SourceBioScience) or mouse αFLAG (M2, Sigma) or rabbit anti-FLAG (GeneScript), and by using goat anti-mouse IgG (H+L) Alexa Flour 488 or 568 and goat anti-rabbit IgG (H+L) Alexa Flour 488 or 568 (Thermo Fisher), as appropriate. Confocal microscopy images were acquired sequentially using a TCS SP5 confocal microscope (Leica) and 100× objective lens using mineral oil immersion and analysed using Leica Application Suite X (Lecia). The transect analysis was based on the method described by Horner *et al*., and different channels from the same image were overlaid using ImageJ [National Institutes for Health (NIH)] [34]. Three five-pixel-wide lines per image were randomly drawn in the MitoTracker or MAVS channel, transecting the area of interest. The pixel intensities along the transects were obtained for both channels of interest and displayed graphically. The three transects were compared individually using Pearson's correlation coefficient and the average coefficient per image was obtained. The graphical representations of the averaged Pearson's *R* values are for at least 10 separate images from 2 independent experiments. For nuclear vs cytoplasmic localizations, multiple images were acquired as above from random fields. The intensity of straining in the nuclear vs cytoplasmic proportions was acquired using these images and Cell Profiler (Broad Institute) according to a published method [35].

Chicken gene transcript quantification

Nasal tissues were dissected, weighed and added to 700 μl of TRIzol reagent (Life Technologies). Tissue was homogenized with a 5 mm stainless steel bead (Qiagen) for 4 min at

Table 2. qPCR and RT-qPCR oligonucleotides [40]

Gene	Fwd (5′ to 3′)	Rev (5′ to 3′)	Probe (5′ to 3′)
IFN-λ	GGCCTTCCTTACCCAAGTCC	CCAGTGCCTCAGTTTCCCAG	SYBR Green
OAS	AAGAACTGGGACTTGGTGGC	CCTTCAGCTCCCAGACTGTG	SYBR Green
RSAD-2	GGACAAGGACGAGACAGTTCC	TCCCGCCTCCTTAAGCATTG	SYBR Green
STAT-1	ACTGCATGCATTGGTGGCCCA	GCTGACGAACTTGCTGCAGGC	SYBR Green
IFN-1	GACAGCCAACGCCAAGC	GTCGCTGCTGTCCAAGCATT	(FAM)CTCAACCGGATCCACCGCTACACC(TAMRA)
IFN-2	CCTCCAACACCTCTTCAACATG	TGGCGTGCGGTCAAT	(FAM)TTAGCAGCCCACACACTCCAAAACACTG (TAMRA)
IFN-γ	GTGAAGAAGGTGAAAGATATCA TGGA	GCTTTGCGCTGGATTCTCA	(FAM)TGGCCAAGCTCCCGATGAACGA(TAMRA)
IL-1β	GCTCTACATGTCGTGTGTGATGAG	TGTCGATGTCCCGCATGA	(FAM)CCACACTGCAGCTGGAGGAAGCC(TAMRA)
IL-6	AACATGCGTCAGCTCCTGAAT	TCTGCTAGGAACTTCTCCA TTGAA	(FAM)AGCAGCACCTCCCTCAAGGCACC(TAMRA)
IL-8	GCCCTCCTCCTGGTTTCAG	TGGCACCGCAGCTCATT	(FAM)TCTTTACCAGCGTCCTACCTTGCGACA(TAMRA)
IL-10	CATGCTGCTGGGCCTGAA	CGTCTCCTTGATCTGCTTGATG	(FAM)CGACGATGCGGCGCTGTCA(TAMRA)
MX	CACTGCAACAAGCAAAGAAGGA	TGATCAACCCCACAAGGAAAA	(FAM)ACAAAGCACACACCCAACTGTCAGCG(TAMRA)
RDLPO-1	TTGGGCATCACCACAAAGATT	CCCACTTGTCTCCGGTCTTAA	(FAM)CATCACTCAGAATTTCAATGGTCCCTCGGG (TAMRA)
RPL13	TCGTGCTGGCAGGATTC	TCGTCCGAGCAAACCTTTTG	(FAM)TAATGCCCGCCAGTTTAAGCTCTTCTAGGC (TAMRA)

20 Hz using a TissueLyser II (Qiagen). RNA was then extracted from centrifuge-clarified homogenate via chloroform and ethanol precipitation. RNA was isolated from cells using a silica-membrane-based RNeasy Mini kit (Qiagen) according to the manufacturer's instructions. Genomic DNA was eliminated using RNase-Free DNase On-Column Digestion (Qiagen). For subsequent analysis of host transcripts by RT-qPCR, cDNA synthesis was performed using Random Primers (Thermo Fisher) and SuperScript III Reverse Transcriptase (Invitrogen). All quantitative PCR (qPCR) was performed using a 7500 Fast and Real-Time PCR System (Applied Biosystems). Twenty microlitres of either TaqMan Universal PCR Master Mix or Power SYBR Green Master Mix were used with 2 µl of cDNA according to the manufacturer's instructions with the primer and probe sets defined in Table 2. Gene expression data were normalized against a stable reference gene and compared against the mock controls using the 2-ΔΔCt method [36]. Reference genes (RDPLO-1 and RSAD) were selected from previous data using GeNorm Reference Gene Selection software (GeNorm) analysis of multiple reference genes on independent samples under identical conditions (Whitehead *et al.*, 2017 under review).

Viral RNA quantification

Quantification of vRNA was performed as previously described [6]. SuperScript III One-Stepreverse transcription-PCR (RT-PCR)system with Platinum *Taq* DNA Polymerase kit (Invitrogen) was usedaccording to the manufacturer's instructions ona 7500 Fast and Real-Time PCR System (Applied Biosystems). Primers and a Taqman probe, specific for a conserved region of the influenza A matrix gene were used as previously published [37] (Spackman et al., 2002). The cycling conditions were: 50 °C for 5 min, 95 °C for 2 min and then 40 cycles of 95 °C for 3 s and 60 °C for 30 s. A T7-transcribed RNA standard of the M gene from A/PR 8/34 (H1N1) was included in each assay to generate a standard curve. Ct values were extrapolated against this curve and the results were expressed as copy numbers of the influenza M gene.

Co-immunoprecipitation of PB1-F2 and ck MAVs or ck IKKβ

Chicken MAVS-V5 or IKKβ-FLAG expression plasmids were co-transfected into DF-1 cells along with PB1-F2 containing a FLAG or V5 tag as appropriate, using lipofectamine 2000 according to the manufacturer's instructions. After incubation for 24 h after transfection, cells were lysed in Pierce Immuoprecipitation Lysis Buffer (Thermo Fisher) and then processed immediately. The lysates were precleared by adding 0.5 mg ml^{-1} of Pierce Protein G Magnetic Beads (Thermo Fisher) and a 12-tube magnetic rack (Qiagen). The samples were incubated overnight at 4 °C with 10 µg ml^{-1} of primary antibody [mouse anti-FLAG (Sigma M2)] or rabbit anti-V5 antibody (Genetex) and then incubated at 4 °C for 6 h with 0.5 mg ml^{-1} of magnetic beads. The beads were magnetically isolated and washed three times in Pierce Immuoprecipitation Lysis Buffer (Thermo Fisher). The beads were then boiled in SDS-loading dye for 10 min and used for Western blot analysis.

VSV-GFP interferon bioassay

The supernatants from three independent experiments involving cells infected with each indicated influenza virus at an m.o.i. of 3 were heated at 60 °C for 30 min to inactivate influenza virus. This was confirmed by performing an in-cell enzyme-linked immunosorbent assay (ELISA) for influenza nucleoprotein. In technical triplicate, the supernatants were twofold serially diluted in complete media on DF-1 cells (4×10^4 cells well^{-1}) in a 96-well opaque white plate (Pierce) and incubated for 12 h. Cells were infected with GFP-tagged vesicular stomatitis virus (VSV-GFP) [38] at an m.o.i. of 3 in Opti-MEM with no phenol red (Thermo). Then, 12 h post-infection, the medium was removed and GFP fluorescence was measured using a GloMax multi-plate reader fluorescence module (Promega). SF9-produced chicken interferon-β was used as a positive control (The Pirbright Institute). No VSV-GFP virus was used to establish background fluorescence and media-only incubations were used to establish maximum fluorescence. The percentage antiviral effect was then calculated using the following formula and displayed graphically:

$$\%\ \text{antiviral effect} = \frac{(\text{sample fluor} - \text{background fluor}) \times 100}{\text{max fluor} - \text{background fluor}} - 100$$

Luciferase reporter assays

For assaying interferon modulation, a pGL3 luciferase (luc) reporter vector containing the promoter regions from chicken IFN-2 upstream of a firefly luc gene was used. For assaying NF-κB activity, a similar reporter vector was used containing six tandem repeats of the NF-κB consensus binding sequence (5′-GGGACTTTCC-3′) upstream of a thymidine kinase (TK) minimal promoter. In triplicate, cells were transfected accordingly with 100 ng of *Renilla* luc pCAGGs expression plasmid, 500 ng chIFN-2-, chMX- or NF-κB luciferase reporter plasmids and 2 µg PB1-F2 protein expression plasmids. For assays involving polyinosinic : polycytidylic acid [poly (I : C)] stimulation, 6 h post-transfection cells were retransfected with 0.25 µg poly I : C (Sigma). After the experimental time point was reached, cells were lysed and read using the Stop and Glo reagents (Promega). Each individual firefly and *Renilla* value was checked for consistency, and then the firefly luciferase signals were normalized to *Renilla* signals.

Cycloheximide chase assay

DF1s were transfected with 250 ng ul^{-1} of the appropriate V5-PB1-F2 or GFP plasmid. Twenty-four hours post-transfection, cells were treated with 100 ug ml^{-1} cycloheximide (Sigma). Samples were collected at appropriate time points by washing with PBS and lysing with Laemmli buffer. Samples were visualized on Western blots using mouse anti-V5 antibody (abcam) and IRDye donkey anti-mouse (800 nm) (LiCor). Actin was used as a loading control and visualized using mouse anti-actin antibody (abcam) with IRDye

donkey anti-mouse (800 nm) (LiCor). GFP was used as a stable protein control. Bands were quantified using ImageJ (NIH) and PB1-F2 was normalized to the actin loading control.

Viral polymerase activity assay

In triplicate, DF-1 cells were transfected with 20 ng of PA, 160 ng of NP, and 80 ng of each of the PB1 and PB2 pCAGGs expression plasmids. Transfection reactions also included 250 ng of chicken-specific viral RNA-dependent RNA polymerase firefly luciferase reporter (described previously [39]) and 100 ng of a *Renilla* luciferase pCAGGs expression plasmid. Cells were incubated for 24 h at either 37 or 41 °C before being lysed in 100 µl of 1× passive lysis buffer (Promega). Plates were frozen for 30 min at −80 °C and defrosted before reading. Then 10 µl of lysate was loaded onto a 96-well opaque white plate (Pierce) and analysed on a GloMax multi-plate reader (Promega) with 50 µl of LARII and Stop and Glo reagents (Promega). Each individual firefly and *Renilla* value was checked for consistency, and then the firefly luciferase signals were normalized to *Renilla* signals.

Viral growth curves

In triplicate, in six-well plates, chicken kidney cells were infected with a virus m.o.i. of 0.0001 1 h at 37 °C. The cells were washed with PBS and incubated at 37 °C with 2 ml of appropriate media containing no serum. Then 500 µl of supernatant was taken at the indicated time points after infection and replenished, and the samples were stored at −80 °C. All samples were titrated via plaque assay on MDCK cells including the input.

Funding information
This work described herein was funded by a The Pirbright Institute studentship grant; BBS/E/00001759, and BBSRC ISP grants; BBS/E/I/00001650, BBS/E/I/00007034 and BBS/E/I/00007038. The funders had no role in study design, data collection, data interpretation, or the decision to submit the work for publication.

Acknowledgements
We would like to acknowledge members of the Influenza Virus and Avian Influenza groups at The Pirbright Institute who supported this work: Dr Dagmara Bialy, Dr Thomas Peacock, Dr Jean-Remy Sadeyen, Dr Pengxiang Chang, Dr Sushant Bhat, Anabel Clements and Joshua Sealy. We thank Dr Muhammed Munir at the University of Lancaster, UK for the kind gift of the VSV-GFP virus for use in the IFN bioassay. PB1-F2 was cloned from viruses (A/mallard/Alb/156/2001 and A/mallard/Alberta/194/92) kindly provided by Professor Robert Webster and Dr Scott Krauss of the St Judes Children's Research Hospital, Memphis, TN, USA. PB1-F2 was cloned from viruses (A/duck/Italy/3139/V06, A/duck/Italy/2253/V06, A/duck/Italy1398/V06, A/duck/Italy/6103/V07) kindly provided by Professor Ilaria Capua, Dr Isabella Monne and Dr Calogero Terregino of the Instituto Zooprofilattico Sperimentalle delle Venezie, Italy.

Conflicts of interest
The authors declare that there are no conflicts of interest.

References

1. **Basuno E, Yusdja Y, Ilham N.** Socio-economic impacts of avian influenza outbreaks on small-scale producers in Indonesia. *Transbound Emerg Dis* 2010;57:7–10.
2. **Govindaraj G, Sridevi R, Nandakumar SN, Vineet R, Rajeev P *et al.*** Economic impacts of avian influenza outbreaks in Kerala, India. *Transbound Emerg Dis* 2018;65:e361–e372.
3. **Qi X, Jiang D, Wang H, Zhuang D, Ma J *et al.*** Calculating the burden of disease of avian-origin H7N9 infections in China. *BMJ Open* 2014;4:e004189.
4. **Vasin AV, Temkina OA, Egorov VV, Klotchenko SA, Plotnikova MA *et al.*** Molecular mechanisms enhancing the proteome of influenza A viruses: an overview of recently discovered proteins. *Virus Res* 2014;185:53–63.
5. **Chen W, Calvo PA, Malide D, Gibbs J, Schubert U *et al.*** A novel influenza A virus mitochondrial protein that induces cell death. *Nat Med* 2001;7:1306–1312.
6. **James J, Howard W, Iqbal M, Nair VK, Barclay WS *et al.*** Influenza A virus PB1-F2 protein prolongs viral shedding in chickens lengthening the transmission window. *J Gen Virol* 2016;97:2516–2527.
7. **Zell R, Krumbholz A, Eitner A, Krieg R, Halbhuber KJ *et al.*** Prevalence of PB1-F2 of influenza A viruses. *J Gen Virol* 2007;88:536–546.
8. **Kamal R, Alymova I, York I.** Evolution and Virulence of Influenza A Virus Protein PB1-F2. *Int J Mol Sci* 2017;19:96.
9. **Klemm C, Boergeling Y, Ludwig S, Ehrhardt C.** Immunomodulatory Nonstructural Proteins of Influenza A Viruses. *Trends Microbiol* 2018;26:624–636.
10. **Košík I, Práznovská M, Košíková M, Bobišová Z, Hollý J *et al.*** The ubiquitination of the influenza A virus PB1-F2 protein is crucial for its biological function. *PLoS One* 2015;10:e0118477.
11. **Leymarie O, Embury-Hyatt C, Chevalier C, Jouneau L, Moroldo M *et al.*** PB1-F2 attenuates virulence of highly pathogenic avian H5N1 influenza virus in chickens. *PLoS One* 2014;9:e100679.
12. **de Jong MD, Simmons CP, Thanh TT, Hien VM, Smith GJ *et al.*** Fatal outcome of human influenza A (H5N1) is associated with high viral load and hypercytokinemia. *Nat Med* 2006;12:1203–1207.
13. **Abdel-Ghafar AN, Chotpitayasunondh T, Gao Z, Hayden FG, Nguyen DH *et al.*** Update on avian influenza A (H5N1) virus infection in humans. *N Engl J Med* 2008;358:261–273.
14. **Yoshizumi T, Ichinohe T, Sasaki O, Otera H, Kawabata S *et al.*** Influenza A virus protein PB1-F2 translocates into mitochondria via Tom40 channels and impairs innate immunity. *Nat Commun* 2014;5:4713.
15. **Chang P, Kuchipudi SV, Mellits KH, Sebastian S, James J *et al.*** Early apoptosis of porcine alveolar macrophages limits avian influenza virus replication and pro-inflammatory dysregulation. *Sci Rep* 2015;5:17999.
16. **Dudek SE, Wixler L, Nordhoff C, Nordmann A, Anhlan D *et al.*** The influenza virus PB1-F2 protein has interferon antagonistic activity. *Biol Chem* 2011;392:1135–1144.
17. **Leymarie O, Meyer L, Tafforeau L, Lotteau V, Costa BD *et al.*** Influenza virus protein PB1-F2 interacts with CALCOCO2 (NDP52) to modulate innate immune response. *J Gen Virol* 2017;98:1196–1208.
18. **Conenello GM, Tisoncik JR, Rosenzweig E, Varga ZT, Palese P *et al.*** A single N66S mutation in the PB1-F2 protein of influenza A virus increases virulence by inhibiting the early interferon response in vivo. *J Virol* 2011;85:652–662.
19. **Varga ZT, Grant A, Manicassamy B, Palese P.** Influenza virus protein PB1-F2 inhibits the induction of type I interferon by binding to MAVS and decreasing mitochondrial membrane potential. *J Virol* 2012;86:8359–8366.
20. **Varga ZT, Ramos I, Hai R, Schmolke M, García-Sastre A *et al.*** The influenza virus protein PB1-F2 inhibits the induction of type I interferon at the level of the MAVS adaptor protein. *PLoS Pathog* 2011;7:e1002067.
21. **Chen S, Cheng A, Wang M.** Innate sensing of viruses by pattern recognition receptors in birds. *Vet Res* 2013;44:82.

22. **Cheng YY, Yang SR, Wang YT, Lin YH, Chen CJ.** Amino Acid Residues 68-71 Contribute to Influenza A Virus PB1-F2 Protein Stability and Functions. *Front Microbiol* 2017;8:692.
23. **Chen CJ, Chen GW, Wang CH, Huang CH, Wang YC *et al.*** Differential localization and function of PB1-F2 derived from different strains of influenza A virus. *J Virol* 2010;84:10051–10062.
24. **Gibbs JS, Malide D, Hornung F, Bennink JR, Yewdell JW.** The influenza A virus PB1-F2 protein targets the inner mitochondrial membrane via a predicted basic amphipathic helix that disrupts mitochondrial function. *J Virol* 2003;77:7214–7224.
25. **Yamada H, Chounan R, Higashi Y, Kurihara N, Kido H.** Mitochondrial targeting sequence of the influenza A virus PB1-F2 protein and its function in mitochondria. *FEBS Lett* 2004;578:331–336.
26. **Reuter A, Soubies S, Härtle S, Schusser B, Kaspers B *et al.*** Antiviral activity of lambda interferon in chickens. *J Virol* 2014;88:2835–2843.
27. **Liniger M, Summerfield A, Zimmer G, Mccullough KC, Ruggli N.** Chicken cells sense influenza A virus infection through MDA5 and CARDIF signaling involving LGP2. *J Virol* 2012;86:705–717.
28. **Reis AL, Mccauley JW.** The influenza virus protein PB1-F2 interacts with IKKβ and modulates NF-κB signalling. *PLoS One* 2013;8:e63852.
29. **Miodek A, Sauriat-Dorizon H, Chevalier C, Delmas B, Vidic J *et al.*** Direct electrochemical detection of PB1-F2 protein of influenza A virus in infected cells. *Biosens Bioelectron* 2014;59:6–13.
30. **Miodek A, Vidic J, Sauriat-Dorizon H, Richard CA, Le Goffic R *et al.*** Electrochemical detection of the oligomerization of PB1-F2 influenza A virus protein in infected cells. *Anal Chem* 2014;86:9098–9105.
31. **Wei P, Li W, Zi H, Cunningham M, Guo Y *et al.*** Epidemiological and molecular characteristics of the PB1-F2 proteins in H7N9 influenza viruses, Jiangsu. *Biomed Res Int* 2015;2015:1–8.
32. **Holmes EC, Lipman DJ, Zamarin D, Yewdell JW.** Comment on "Large-scale sequence analysis of avian influenza isolates". *Science* 2006;313:1573b.
33. **Marais R, Light Y, Paterson HF, Marshall CJ.** Ras recruits Raf-1 to the plasma membrane for activation by tyrosine phosphorylation. *Embo J* 1995;14:3136–3145.
34. **Horner SM, Liu HM, Park HS, Briley J, Gale M.** Mitochondrial-associated endoplasmic reticulum membranes (MAM) form innate immune synapses and are targeted by hepatitis C virus. *Proc Natl Acad Sci USA* 2011;108:14590–14595.
35. **Carpenter AE, Jones TR, Lamprecht MR, Clarke C, Kang IH *et al.*** CellProfiler: image analysis software for identifying and quantifying cell phenotypes. *Genome Biol* 2006;7:R100.
36. **Pfaffl MW.** A new mathematical model for relative quantification in real-time RT-PCR. *Nucleic Acids Res* 2001;29:45e–45.
37. **Spackman E, Senne DA, Myers TJ, Bulaga LL, Garber LP *et al.*** Development of a real-time reverse transcriptase PCR assay for type A influenza virus and the avian H5 and H7 hemagglutinin subtypes. *J Clin Microbiol* 2002;40:3256–3260.
38. **Berger Rentsch M, Zimmer G.** A vesicular stomatitis virus replicon-based bioassay for the rapid and sensitive determination of multi-species type I interferon. *PLoS One* 2011;6:e25858.
39. **Moncorgé O, Long JS, Cauldwell AV, Zhou H, Lycett SJ *et al.*** Investigation of influenza virus polymerase activity in pig cells. *J Virol* 2013;87:384–394.
40. **Giotis ES, Robey RC, Skinner NG, Tomlinson CD, Goodbourn S *et al.*** Chicken interferome: avian interferon-stimulated genes identified by microarray and RNA-seq of primary chick embryo fibroblasts treated with a chicken type I interferon (IFN-α). *Vet Res* 2016;47:75.